

Engineering chemically abrupt high- k metal oxide/silicon interfaces using an oxygen-gettering metal overlayer

Hyounsub Kim^{a)} and Paul C. McIntyre

Department of Materials Science and Engineering, Stanford University, Stanford, California 94305

Chi On Chui and Krishna C. Saraswat

Department of Electrical Engineering, Stanford University, Stanford, California 94305

Susanne Stemmer

Materials Department, University of California, Santa Barbara, California 93106-5050

(Received 29 March 2004; accepted 3 June 2004)

High- k metal oxide gate dielectrics may be required to extend Moore's law of semiconductor device density scaling into the future. However, growth of a thin SiO₂-containing interface layer is almost unavoidable during the deposition of metal oxide films onto Si substrates. This limits the scaling benefits of incorporating high- k dielectrics in future transistors. A promising approach, in which oxygen-gettering metal overlayers are used to engineer the thickness of the SiO₂-based interface layer between metal oxide and Si substrate *after* deposition of the metal oxide layer, is reported. Using a Ti overlayer with high solubility for oxygen on ZrO₂ or HfO₂ dielectrics, the effective removal of the low- k interface layer at 300 K has been confirmed by electron microscopy and spectroscopy techniques. Significant enhancement of the gate capacitance density, while retaining low leakage current densities, has also been demonstrated for these interface-engineered high- k gate stacks. © 2004 American Institute of Physics. [DOI: 10.1063/1.1776636]

I. INTRODUCTION

There is now intense worldwide scientific and technological interest in the topic of metal oxide/semiconductor interfaces and much of it was prompted by the search for high permittivity (high- k) dielectric materials to replace SiO₂ as a gate insulator in metal-oxide-semiconductor field effect transistors (MOSFETs). Such a replacement is likely required in order to achieve sufficiently high gate capacitance densities for reliable device operation as MOSFETs are scaled down to very small lateral dimensions (gate lengths <30 nm) in the coming years. High- k dielectrics are, therefore, a critical enabler of the continuation of Moore's law, the steady increase in silicon device areal density that has occurred during the past 30–40 years, and has led to enormous increases in computing power and portability.

Selection of a replacement gate insulator with dielectric constant greater than that of SiO₂ ($k_{\text{SiO}_2}=3.9$) is complicated by the fact that very few materials exhibit the desired combination of high polarizability, large band gap, and excellent thermal stability in contact with Si.¹ Most of the recent research has focused on a small number of metal oxides: HfO₂, ZrO₂, La₂O₃ etc., and their alloys with SiO₂ and Al₂O₃. Deposition of a metal oxide (MO) film on a Si substrate is, however, often accompanied by the growth of a thin SiO₂-containing interfacial layer (IL) that results from oxidation of the Si surface. The IL forms because the metal oxide layer must usually be deposited in an oxygen-rich ambient in order to achieve the correct metal-to-oxygen stoichiometry. Furthermore, atomic layer deposition (ALD), one of

the most promising methods for controlled deposition of ultrathin metal oxides onto Si, requires a high density of surface sites for precursor adsorption.² Experimentally, it is found that a SiO₂-based surface passivation provides an ideal template for ALD of high- k metal oxides on Si.^{3,4} It is, therefore, a common practice to passivate the Si surface with a very thin SiO₂ film prior to MO deposition by ALD. The IL, whether intentionally added or formed as a result of MO deposition itself, can have a profound effect on the behavior of the MO/IL/Si structure. Because capacitances in series add in reciprocal fashion, the dielectric properties of the IL often dominate the characteristics of the entire gate stack, thus limiting the scaling benefits of incorporating the high- k layer in the device. For this reason, there is great interest in developing approaches for reducing the thickness of the IL and, perhaps, eliminating it entirely.

In this paper, we report on a method for removing the SiO₂-based IL after deposition of HfO₂ and ZrO₂ gate dielectrics on Si substrates, and we describe the resulting MO/Si interface structures and electrical properties. Our approach makes use of the thermodynamic properties of reactive metals which can dissolve large amounts (>10 at.%) of oxygen without forming a new oxide phase. We show that Ti is a suitable metal for this purpose. By depositing thin films of Ti onto a stable MO film which has a high permeability for oxygen, the IL between the MO film and Si substrate can be altered and, in some cases, removed. Oxygen ions from the IL diffuse across the continuous HfO₂ and ZrO₂ dielectric layers and dissolve into the Ti overlayer at temperatures near 300 K. Silicon atoms initially in the IL appear to be reincorporated in the surface of the Si substrate as the SiO₂-based IL decomposes.

^{a)}Author to whom correspondence should be addressed; electronic mail: hsubkim@stanford.edu

II. EXPERIMENT

Approximately 1.5 nm thick chemical oxides (SiO_2) on *p*-type $\langle 100 \rangle$ Si wafers having 1–10 (Ω cm) resistivity were used as substrates. Depositions of ~ 3.9 nm ZrO_2 and ~ 3.6 nm HfO_2 were performed at 300°C using alternating surface-saturating reactions of metal chlorides (ZrCl_4 and HfCl_4 , respectively) and H_2O in a cold-wall-type, high vacuum-base pressure ALD system.⁵ Each precursor was pulsed for 2 s and N_2 purging was followed for 30 and 60 s after H_2O and HfCl_4 pulsing, respectively. The base pressure of the system is in mid- 10^{-8} -Torr range and the process pressure was maintained at 0.5 Torr during ALD. Various process results, such as linear growth rate, independence of growth rate on precursor pulse and purging duration, and near-perfect step coverage on high aspect-ratio structures, confirmed that the deposition processes used to synthesize ZrO_2 and HfO_2 in these experiments were in the true ALD regime. As-deposited ALD- HfO_2 films were found to be amorphous by electron diffraction, whereas the ZrO_2 films were polycrystalline (with grain size comparable to the film thickness) and had the tetragonal crystal structure.

In making simple MOS capacitors using ALD high-*k* films, various sizes of metal electrodes (50 nm Pt, 100 nm Al, and 50 nm Pt/30 nm Ti) were *ex situ* deposited at room temperature by the shadow mask technique using an *e*-beam evaporation system. A thin film of Pt was used to cap the reactive Ti metal electrodes to prevent its subsequent oxidation on exposure to air. In order to minimize the sample series resistance, the backside of each specimen was scratched to remove any native oxide using a diamond scribe and was coated with a ~ 100 nm thick Al film. MOS capacitor samples were studied electrically using capacitance-voltage (CV) and current-voltage (IV) analysis both before and after a 300°C , 4% H_2 /96% N_2 forming gas anneal. Such low temperature hydrogen anneals are typically performed to reduce the density of interface states in MOS devices through passivation of dangling bonds at the SiO_2 /Si interface. The actual sizes of the capacitors were calibrated using an optical microscope. The final distribution of the measured capacitance values showed less than $\pm 5\%$ variation for each of the samples investigated. These small variations in capacitance are consistent with shadowing effects which occur during the metal electrode deposition step. CV measurements were performed in parallel mode using an HP4284A precision LCR meter at various frequencies (10, 100, and 800 kHz). The capacitors were swept from inversion to accumulation and back to check the amount of hysteresis. For IV measurements, a Keithley 230 programmable voltage source and a 6512 programmable electrometer were used. Since the Si substrates used in this work were doped with low amounts of *p*-type impurities, the gate electrode was negatively biased and swept under a gate injection condition.

Transmission electron microscopy (TEM) was used to study the interface structures in the dielectric stacks after completion of all electrical measurements. High resolution TEM analyses were performed using a Philips FEG CM20 microscope operating at 200 kV accelerating voltage, which offers a point-to-point spatial resolution of 2.4 Å. The local

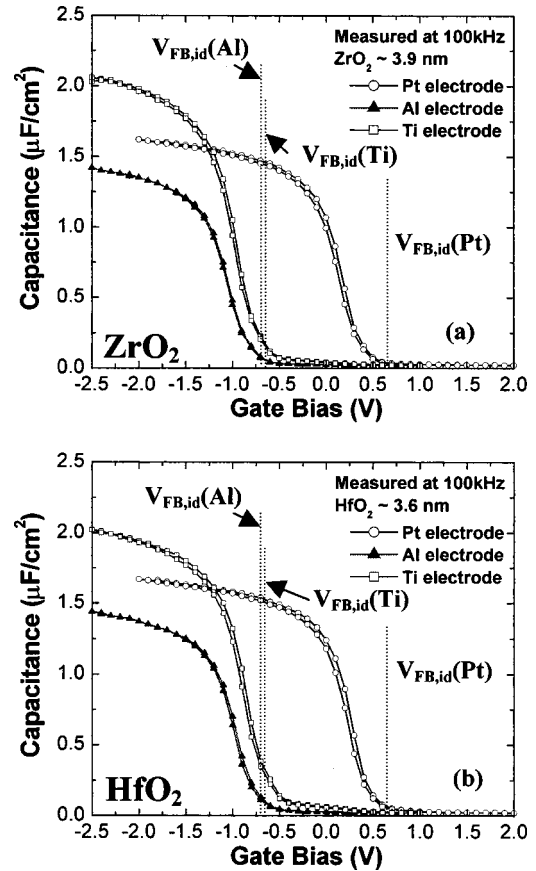


FIG. 1. CV data obtained from Al-, Pt-, and Ti-electroded (a) ZrO_2 and (b) HfO_2 high-*k* capacitors on *p*-type Si substrates after 300°C , 30 min forming gas anneal; measurements taken at 100 kHz frequency and both bias sweep directions are shown.

composition within the metal/dielectric Si stack was characterized by high-angle annular dark field (HAADF) imaging and electron energy loss spectroscopy (EELS) in scanning transmission electron microscopy (STEM). For HAADF imaging and EELS, a JEOL 2010F field-emission transmission electron microscope equipped with annular dark field detectors and a Gatan imaging filter was used. The microscope was operated in STEM mode, using a probe size of ~ 0.2 nm. The HAADF image was used to position the small electron probe at different locations across the gate stack to record the EELS spectra. EELS O *K* and Ti *L* edges were recorded with an energy dispersion of 0.3 eV/channel and 10 s acquisition time.

III. RESULTS AND DISCUSSIONS

A. Electrical and microstructural characterization

Comparison of CV plots obtained from Ti/high-*k*/Si capacitors to those of Pt/high-*k*/Si and Al high-*k* Si capacitors after forming gas anneal (Fig. 1) indicates that the capacitance density of the Ti-electrode capacitors was significantly higher even though all capacitor sets were processed identically except for the identity of the gate electrode. The equivalent oxide thickness (EOT) is an important figure of merit for the gate capacitance density:

$$\text{EOT} = (k_{\text{SiO}_2} d / k_{\text{eff}}), \quad (1)$$

where d is the physical thickness of the dielectric stack and k_{eff} is its effective dielectric constant. The measured EOT is significantly smaller for Ti-electroded high- k capacitors than for otherwise identical Pt-electroded samples. This EOT difference was also observed, with similar magnitude, for as-deposited Ti-electroded capacitors which were not given a forming gas anneal (not shown). For all samples shown in the figure, the high- k layers (ZrO_2 and HfO_2) were ~ 3.9 and ~ 3.6 nm in thicknesses, respectively. The EOT values extracted directly from the accumulation capacitance of the Ti-electroded capacitors (without quantum mechanical corrections) were 1.6 nm for ZrO_2 and 1.7 nm for HfO_2 dielectric layers. In contrast, the Pt-electroded EOT values were ~ 2.1 nm for ZrO_2 and HfO_2 . In the case of Al-electroded capacitors, EOT values were substantially larger (2.4–2.5 nm) for both ZrO_2 and HfO_2 .

In addition to variations in accumulation capacitance density among the samples in Fig. 1, the Al- and Ti-electroded capacitors exhibit CV curves, which are shifted with respect to the Pt-electrode data. This shift in flat band voltage is in good quantitative agreement with the difference in the reported work functions of Al and Ti compared to that of Pt. The theoretically predicted⁶ flat band voltages of the Al-, Ti-, and Pt-electroded capacitors are -0.71 , -0.66 , and $+0.66$ V, respectively, as shown in Fig. 1.

The CV data in Fig. 1 show both bias sweep directions, and there is minimal hysteresis for the capacitance values obtained. Leakage current densities measured across the metal electrode/high- k /Si capacitors after the forming gas anneal are shown in Fig. 2. As a result of the smaller equivalent electrical thickness and the smaller barrier height of Ti/high- k /Si stacks, their leakage current densities are consistently higher than those of the Pt/high- k /Si capacitors. For Al-electroded capacitors, relatively high leakage currents were measured due to the decrease of the barrier height and also, perhaps, due to an increase in the density of trapping sites formed by the Al/metal oxide interfacial reaction.

In terms of the absolute value of their leakage current densities, the Ti-electroded capacitors are quite promising. The Ti/ HfO_2 /Si samples, with $\text{EOT} = \sim 1.7$ nm, have a leakage current density of $\sim 5 \times 10^{-5}$ A/cm² at 1 V from the flat band condition. This current is approximately four orders of magnitude smaller than that measured across high-quality SiO_2 films of the same EOT,⁷ a consequence of the larger physical thickness of the high- k layer which minimizes direct band-to-band tunneling conduction.

The reason for the reduced EOT value of the Ti-electroded capacitors is evident in both high resolution TEM (HRTEM) and annular dark field STEM images obtained from cross-section samples. The HRTEM images in Fig. 3 compare the layer structures present in HfO_2 gate stacks with Ti and Al electrodes. The amorphous, light contrast layer, which is present at the dielectric Si interface in the Al-electroded sample, was substantially thinned and, possibly, removed entirely from the Ti-electroded sample.

A similar result was obtained from STEM/EELS studies of the Al- and Ti-electroded ZrO_2 gate stacks. For thin

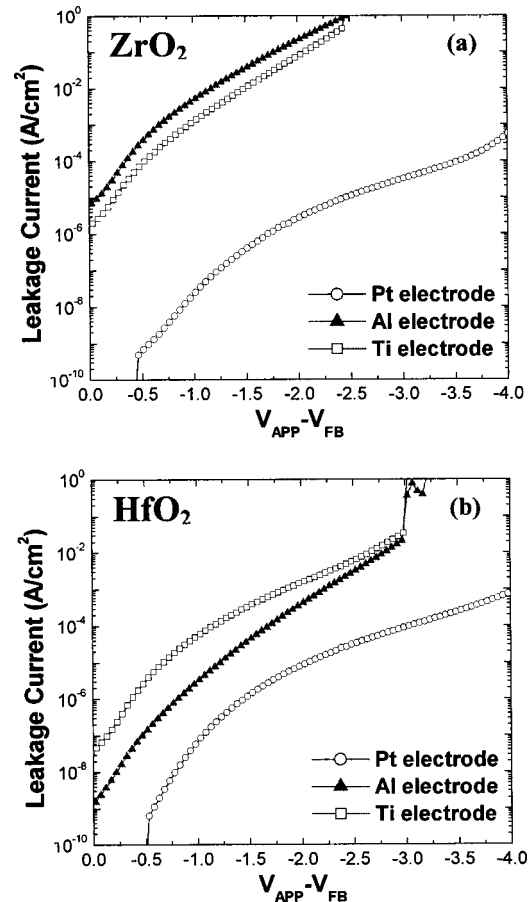


FIG. 2. IV data measured from Al-, Pt-, and Ti-electroded (a) ZrO_2 and (b) HfO_2 high- k capacitors on p -type Si substrates after 300°C , 30 min forming gas anneal; gate voltage shown in referenced to the flat band voltage for each electrode material.

samples, the contrast in the high-angle annular dark field image in STEM is strongly dependent on the atomic number Z , and thus provides a chemically sensitive image that reflects composition variation across the gate stack.⁸ In particular, low- Z amorphous layers, such as SiO_2 , appear dark in these images, whereas Hf- or Zr-based high- k layers appear bright. The HAADF image of the Al-electroded ZrO_2 sample in Fig. 4(a) shows the typical dark contrast band associated with the low-average atomic number, SiO_2 -based IL present between the high- k film and Si substrate. Its thickness is similar to that of the chemical oxide present on the Si substrate surface prior to ALD growth of the high- k layer. In addition, a thinner dark-contrast band is visible at the Al/ ZrO_2 interface. EELS showed that the upper interfacial layer contains oxygen. The presence of this layer, which is also evident in conventional TEM images from this sample, suggests reaction between the Al electrode and ZrO_2 high- k layer, as reported by others.⁹ The greater thermodynamic stability of Al_2O_3 relative to its metal in comparison to ZrO_2 and Zr (Ref. 10) may explain the apparent reactivity of the Al/ ZrO_2 samples, although further work is required to unambiguously identify the low-average atomic number phase formed at this interface. This interfacial reaction may also account for the larger leakage current densities and inferior CV characteristics of the Al/ ZrO_2 /Si capacitors.

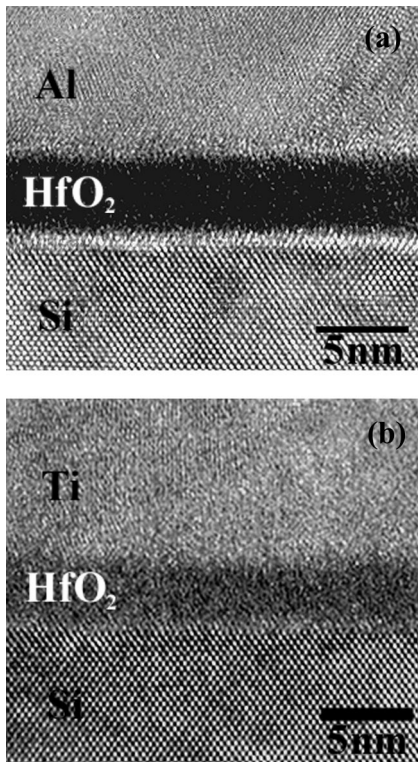


FIG. 3. High resolution cross-sectional TEM images of (a) Al/HfO₂/SiO₂/Si and (b) Pt/Ti/HfO₂/Si gate stacks after 300°C, 30 min forming gas anneal.

In contrast to the Al-electrode results, the HAADF image in Fig. 4(b) shows the absence of a dark-contrast interfacial region in the Ti/ZrO₂/Si capacitor structure. No evidence for a low atomic number interface layer is found in the Ti-electroded gate stacks. EELS spectra obtained from the same region indicate that a significant oxygen concentration is present in the Ti overlayer and that no Ti is detected at the ZrO₂/Si interface or in the ZrO₂ layer within the detection limit of the method [Fig. 4(c)]. This is consistent with reports from the literature of a very small solubility (<4 at.% 1200°C) of Ti in ZrO₂.¹¹

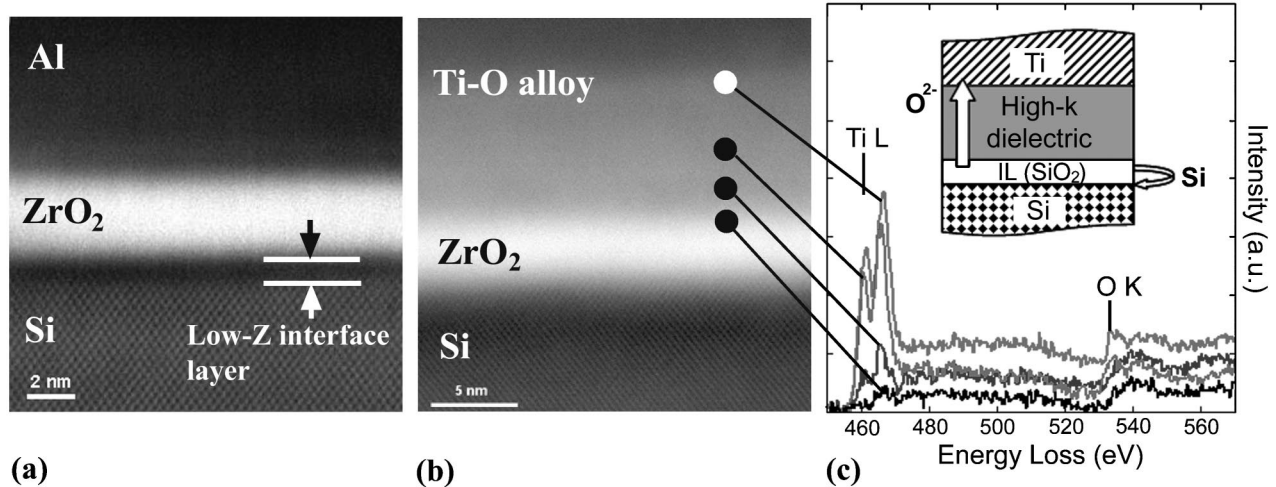
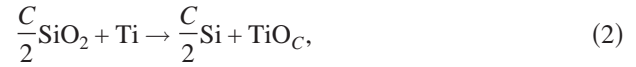


FIG. 4. (a) High-angle annular dark field image of Al/ZrO₂/SiO₂/Si gate stack, (b) high-angle annular dark field image, and (c) accompanying local EELS spectra, showing Ti L₂₃ edges (~456 eV) and O K edges (~532 eV) recorded at different locations in the Pt/Ti/ZrO₂/Si gate stack after 300°C, 30 min forming gas anneal; the EELS spectra were recorded at the location indicated in the HAADF image. The inset schematic shows the proposed process of oxygen ion diffusion across the ZrO₂ layer and incorporation of Si into the substrate surface during interfacial SiO₂ decomposition.

B. Thermodynamic analysis

A thermodynamic driving force exists for decomposition of the SiO₂ IL in these structures and incorporation of the liberated oxygen atoms in the Ti overlayer. The overall chemical reaction for this process can be written as follows:



where TiO_C is the Ti-O alloy overlayer. In reaction (2), the Si atoms are assumed to reincorporate into the underlying single crystal substrate during decomposition of the IL. This is consistent with our TEM observations, which failed to detect any evidence of a defective Si layer at the metal oxide/silicon interface of the Ti-electroded capacitors. Using published data for the Gibbs free energy of formation of SiO₂ from its elements¹² and the equilibrium oxygen vapor pressure Ti-O alloys of varying stoichiometry,¹³ one can show that the standard Gibbs free energy change associated with reaction (2) is large and negative for all values of *C* upto the oxygen solubility limit in α -Ti ($C < 0.49$).¹⁴

First the Dehum-Margules equation¹⁵ was used to determine the integral Gibbs free energy of formation of TiO_C (an interstitial alloy of oxygen in α -Ti):

$$\Delta G_{f,\text{TiO}_C}^0 = (RT/2) \int_0^C \ln P_{\text{O}_2}^{\text{eq}} dC, \quad (3)$$

where *R* is the gas constant, *T* is the absolute temperature, and $P_{\text{O}_2}^{\text{eq}}$ is the equilibrium vapor pressure of oxygen above α -Ti for varying dissolved oxygen concentrations. Original data by Komarek and Silver have been fitted by Wang and Kim¹³ to give

$$\ln P_{\text{O}_2}^{\text{eq}} = 21.34 + 12.45C + 2 \ln[C/(1 - C)] - 131\,200/T. \quad (4)$$

The standard Gibbs free energy of formation of SiO₂ from its elements¹² was subtracted from $\Delta G_{f,\text{TiO}_C}^0$ to give the free en-

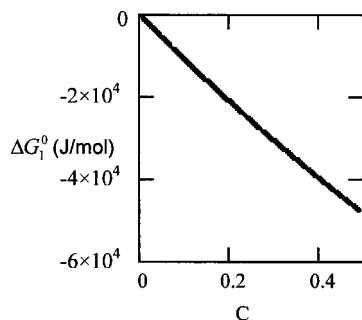


FIG. 5. Gibbs free energy change of the reaction $(C/2)\text{SiO}_2 + \text{Ti} \rightarrow (C/2)\text{Si} + \text{TiO}_x$, as a function of C at $T=573$ K.

ergy change of reaction (2) at $T=573$ K. This quantity is plotted as a function of C in Fig. 5 for $T=573$ K, the maximum temperature to which the Ti-electroded capacitors were exposed in this study. Reaction (2) experiences a strong driving force to proceed for all temperatures of interest in semiconductor processing. Similar large thermodynamic driving forces exist for other IL and metal overlayer combinations in the limit that the metal layer is initially highly pure. However, the Ti overlayer is unusual because of its very large capacity for dissolving oxygen compared to other metals.

The ability of Ti films to decompose native silicon oxide layers onto which they are directly deposited has previously been demonstrated.^{16,17} The reaction has been reported to occur via low temperature dissolution of oxygen into the Ti overlayer, similar to reaction (2). However, in the case presented here, the decomposition of SiO_2 and dissolution of oxygen require oxygen ion diffusion across a high- k metal oxide layer that is interposed between the Ti and the oxidized Si surfaces. This process is depicted schematically in the inset to Fig. 4(c).

Oxygen ion diffusion in bulk metal oxide crystals, such as ZrO_2 and HfO_2 , is typically mediated by oxygen vacancies. However, grain boundary diffusion may be significant in the fine-grained polycrystalline samples such as our ALD- ZrO_2 thin films.¹⁸ Diffusion of oxygen along paths of high excess volume is also possible in thin amorphous films such as the ALD- HfO_2 films used in our experiments. Although the experimental results obtained to date do not allow us to quantify the relative contributions of these oxygen transport mechanisms to the process of IL decomposition, it is evident that the kinetics of oxygen diffusion are quite rapid, even at temperatures near 300 K. For a maximum diffusion time on the order of minutes and a metal oxide film thickness of 4 nm, an oxygen diffusivity across the metal oxide films of order 10^{-14} – 10^{-16} cm^2/s can be estimated for the ALD- ZrO_2 and ALD- HfO_2 films. To our knowledge, the oxygen diffusivities in amorphous HfO_2 and undoped tetragonal ZrO_2 have not yet been measured; however, data from yttria-stabilized cubic zirconia are available.^{19,20} When extrapolated to 300 K, these reported results are consistent with an oxygen diffusivity through the high- k layer of order 10^{-16} cm^2/s , close to the lower bound of the range of diffusivities estimated from our own observations.

Studies of otherwise identical ALD films of 12–15 nm thickness with Ti electrodes indicated that a lower-atomic-

number amorphous layer of ~ 0.8 nm thickness (half of the original chemical oxide thickness) was present at the high- k /Si interface after the 300°C forming gas anneal (not shown here). These observations indicate that the rate of IL decomposition can be slowed appreciably by increasing the distance over which oxygen must diffuse to reach the Ti overlayer.

In addition to decomposition of the SiO_2 IL, dissolution of oxygen into the Ti electrode layer will remove oxygen from the interposed metal oxide film. Such oxygen loss may contribute fixed charge and bulk trap states of the dielectric. Zirconia and structurally similar metal oxides are prone to oxygen deficiency through formation of oxygen vacancies under conditions of low oxygen activity. Insight into possible electrode-induced reduction of the high- k film can be obtained by careful analysis of the electrical data. Oxygen vacancies are generally donor-type charged defects in metal oxides and would be expected to produce positive fixed charge in oxygen-deficient high- k films. Because the reduction which produce oxygen vacancies also produce electrons as charge-compensating species,²¹ metal oxide films with substantial oxygen deficiency are also found to exhibit a significant frequency dispersion and large loss-factor resulting from their enhanced electronic conductivity.²²

The fixed charge present in the dielectric stacks can be estimated from the flat band voltage measured by CV analysis. The identical metal work functions as determined by spectroscopy were assumed in calculating the density fixed charge, although it may not be correct for metal/high- k gate stacks. The results obtained from both Ti-electroded and Pt-electroded high- k capacitors are consistent with a net positive fixed charge density of $\sim 10^{12}$ cm^{-2} . This indicates that the presence of an oxygen-gettering Ti overlayer does not lead to a significant increase in the dielectric fixed charge over that present with less reactive Pt electrodes. The measured fixed charge areal density is consistent with a volumetric charge density of 10^{18} – 10^{19} cm^{-3} in the ALD- HfO_2 and ALD- ZrO_2 , independent of electrode material.

In previous studies of the effects of oxygen stoichiometry on the behavior of high- k metal oxide films,²² we have shown that MOS capacitor measurements will detect high leakage current densities and a very large frequency dispersion of the dielectric constant when significant oxygen deficiency (~ 10 at.%) occurs. The leakage current densities obtained in the present experiments on Ti-electroded MO dielectrics are low for the measured EOT, and minimal frequency dispersion was detected (Fig. 6) after correction of the CV data for the series resistance of the Si substrates.²³ The slight dispersion seen in Fig. 6 is almost identical in magnitude to that observed for identically processed low-leakage Ti-electroded SiO_2 capacitors with 10 nm dielectric thickness, suggesting that it is a property of the Ti-O electrode layer rather than the dielectric. We conclude, therefore, that any oxygen deficiency induced in the metal oxide dielectrics by their equilibration with the Ti electrode layer is too small to be detected in the present capacitor measurements.

With complete removal of the low- k IL, one might expect that the EOT of Ti-electroded samples should decrease from the value measured for Pt-electroded devices by a fac-

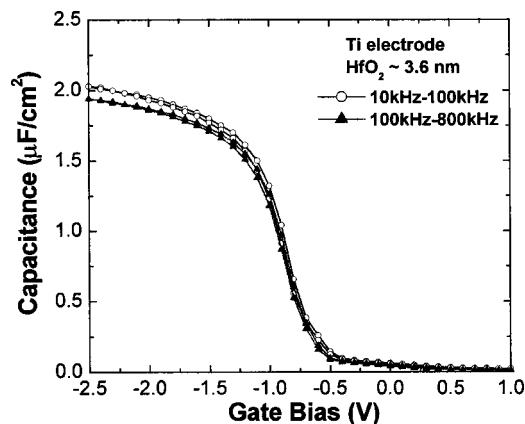


FIG. 6. CV plots for a representative Ti-electroded HfO_2 high- k capacitor after frequency correction for the series resistance of the Si substrate; data collected at 10, 100, and 800 kHz.

tor of ~ 1.5 nm. However, the decrease of EOT obtained from the CV curves was only ~ 0.5 nm for both high- k dielectrics. This more modest, but still significant, EOT reduction may result from several different factors. If all of the Si present in the initial IL is epitaxially regrown onto the surface of the underlying Si substrate during IL decomposition, then it is reasonable to expect the formation of ~ 1.2 nm of undoped Si at the wafer surface which could contribute an EOT of ~ 0.4 nm to the IL-free gate stack. It is also possible that some of the Si initially present in the IL is incorporated in the high- k layer, thus lowering its dielectric constant. The incorporation of large amounts of oxygen in the Ti electrode may also reduce its conductivity substantially and add to the EOT of these devices. If so, etching the Ti-O electrode layer to remove it after IL decomposition may be a fruitful approach for engineering ultralow EOT gate stacks on Si substrates. Further experiments are underway to examine these possibilities.

IV. CONCLUSIONS

We have reported a promising approach for engineering the thickness of the SiO_2 -based interface layer between metal oxide films and silicon after deposition of the metal oxide layer. We have shown that a Ti overlayer, which exhibits a very high oxygen solubility, can effectively getter oxygen from the interface layer through an interposed metal oxide high- k layer, thus decomposing SiO_2 and reducing the interface layer thickness in a controllable fashion. The kinetics of the process appears to be limited by the oxygen permeability of the interposed metal oxide film. Electrical characteristics of low-EOT MOS capacitors fabricated in this manner are very promising. Minimal CV hysteresis and dispersion are

observed and the leakage current densities are low for the measured EOT values. This method for engineering the thickness of the interface layer between silicon and metal oxide films may be extendable to other materials systems and applications beyond MOS transistors and capacitors.

ACKNOWLEDGMENTS

This work was supported in part by the National Science Foundation (Grant No. DMR0072134), by the DARPA HGI program, and by the Semiconductors Research Corporation (Grant No. 1015.001). H. K. acknowledges financial support from a Mayfield Group Stanford Graduate Fellowship. S. S. gratefully acknowledges the use of the TEM/STEM facilities at the RRC of the University of Illinois at Chicago.

- ¹G. D. Wilk, R. M. Wallace, and J. M. Anthony, *J. Appl. Phys.* **89**, 5243 (2001).
- ²M. Leskelä and M. Ritala, *Thin Solid Films* **409**, 138 (2002).
- ³M. L. Green, M.-Y. Ho, B. Busch, G. D. Wilk, T. Sorsch, T. Conard, B. Brijis, W. Vandervorst, P. I. Räisänen, D. Muller, M. Bude, and J. Grazul, *J. Appl. Phys.* **92**, 7168 (2002).
- ⁴C. M. Perkins, B. B. Triplett, P. C. McIntyre, K. C. Saraswat, S. Haukka, and M. Tuominen, *Appl. Phys. Lett.* **78**, 2357 (2001).
- ⁵H. Kim, P. C. McIntyre, and K. C. Saraswat, *Appl. Phys. Lett.* **82**, 106 (2003).
- ⁶E. H. Nicollian and J. R. Brews, *MOS (Metal Oxide Semiconductor) Physics and Technology* (Wiley, New Jersey, 2003).
- ⁷G. Timp *et al.*, *Tech. Dig. - Int. Electron Devices Meet.* **1998** 615.
- ⁸J. C. H. Spence, *High-Resolution Electron Microscopy*, 3rd ed. (Oxford University Press, Oxford, 2003).
- ⁹D. A. Muller and G. D. Wilk, *Appl. Phys. Lett.* **79**, 4195 (2001).
- ¹⁰C. H. P. Lupis, *Chemical Thermodynamics of Materials* (North-Holland, New York, 1983).
- ¹¹R. F. Domagala, S. R. Lyon, and R. Ruh, *J. Am. Ceram. Soc.* **56**, 584 (1973).
- ¹²I. Barin and O. Knacke, *Thermochemical Properties of Inorganic Substances* (Springer, Berlin, 1977).
- ¹³W. E. Wang and Y. S. Kim, *J. Nucl. Mater.* **270**, 242 (1999); K. L. Komarek and M. Silver, in *Thermodynamics of Nuclear Materials* (IAEA, Vienna, 1962), p. 749.
- ¹⁴L. Murray and H. A. Wriedt, *Phase Diagrams of Binary Titanium Alloys* (ASM International, Ohio, 1987).
- ¹⁵O. Kubaschewski, C. B. Alcock, and P. J. Spencer, *Materials Thermochemistry* (Pergamon, Oxford, 1993), p. 35.
- ¹⁶M. Liehr, F. K. LeGoues, G. W. Rubloff, and P. S. Ho, *J. Vac. Sci. Technol. A* **3**, 983 (1985).
- ¹⁷J. C. Barbour, A. E. M. J. Fischer, and J. F. van der Veen, *J. Appl. Phys.* **62**, 2582 (1987).
- ¹⁸U. Brossmann, R. Wurschum, U. Sodervall, and H. E. Schaefer, *J. Appl. Phys.* **85**, 7646 (1999).
- ¹⁹S. F. Palguez, V. K. Gilderman, and A. D. Neujmin, *J. Electrochem. Soc.* **122**, 745 (1975).
- ²⁰K. Sasaki and J. Maier, *Solid State Ion. Diffus. React.* **134**, 303 (2000).
- ²¹F. A. Kröger and H. J. Vink, *Solid State Phys.-Adv. Res. Appl.* **3**, 307 (1956).
- ²²S. Ramanathan, D. A. Muller, G. D. Wilk, C. M. Park, and P. C. McIntyre, *Appl. Phys. Lett.* **79**, 3311 (2001).
- ²³K. J. Yang and C. M. Hu, *IEEE Trans. Electron Devices* **46**, 1500 (1999).